Transient Floral Change and Rapid Global Warming at the Paleocene-Eocene Boundary

Scott L. Wing,[1]* Guy J. Harrington,[2] Francesca A. Smith,[1,3] Jonathan I. Bloch,[4] Douglas M. Boyer,[5] Katherine H. Freeman[3]

Rapid global warming of 5° to 10°C during the Paleocene-Eocene Thermal Maximum (PETM) coincided with major turnover in vertebrate faunas, but previous studies have found little floral change. Plant fossils discovered in Wyoming, United States, show that PETM floras were a mixture of native and migrant lineages and that plant range shifts were large and rapid (occurring within 10,000 years). Floral composition and leaf shape and size suggest that climate warmed by ~5°C during the PETM and that precipitation was low early in the event and increased later. Floral response to warming and/or increased atmospheric CO_2 during the PETM was comparable in rate and magnitude to that seen in postglacial floras and to the predicted effects of anthropogenic carbon release and climate change on future vegetation.

At the beginning of the Eocene Epoch ~55.8 million years ago, global temperatures increased by 5° to 10°C over a period of ~10 to 20 thousand years (ky) then returned to warm background climates over the succeeding ~100 ky (*1*–*4*). This event, the Paleocene-Eocene Thermal Maximum (PETM) (*5*), coincided with a global negative carbon isotope excursion (CIE) and calcium carbonate dissolution in the deep ocean, which are consistent with a large release of ^{13}C-depleted carbon to the ocean and atmosphere (*6*). Several sources have been proposed for this carbon: ocean-floor clathrates (*7*), thermogenic methane (*8*), and burning of peat and/or shallowly buried coals (*9*).

Biotic events at the PETM include mass extinction among benthic foraminifera (*10*), changes in the latitudinal range and species composition of marine plankton (*11*, *12*), and shifts in the taxonomic and trophic composition of terrestrial vertebrate faunas, probably after dispersal over high-latitude land bridges (*13*, *14*). Although the distribution and diversity of terrestrial plants are strongly influenced by climate today, previous work has shown little mega- or palynofloral change across the Paleocene-Eocene interval (*15*–*19*). Here we report terrestrial megafloras from the PETM and use them to infer change in the climate and floral composition in the interior of North America.

Geological framework. Our data come from the upper Fort Union and lower Willwood formations in the Cabin Fork drainage, southeastern Bighorn Basin, Wyoming, United States (~43.96°N, 107.65°W) (Fig. 1). These sediments were deposited by small fluvial systems near the margin of a subsiding intermontane basin, and they preserve a suite of environments including small channels, floodplain paleosols and swamps, and abandoned channel fills. We measured strata with a Jacob's staff and sighting level, then correlated sections by tracing beds with a differential Global Positioning System to create a stratigraphic and biostratigraphic framework with ~1-m resolution (Fig. 2).

Two lines of evidence establish the PETM age of these strata: mammalian biostratigraphy and $\delta^{13}C$ of paleosol organic matter. Fossil mammals indicating the late Paleocene Clarkforkian North American Land Mammal Age (NALMA) were found from 5 to 22 m below the top of the Fort Union formation (Fig. 2). The main fossiliferous layer is a laterally extensive, ferruginous, grit-pebble conglomerate that has produced >200 specimens and 11 species. The presence of *Copecion*, an abundance of *Phenacodus* and *Ectocion*, and the absence of *Hyracotherium* indicate that this fauna belongs to the latest Clarkforkian zone Cf-3 (*20*, *21*). The earliest Eocene mammals (Wasatchian NALMA, the Wa-0 zone), which occur within the CIE in other areas (*19*, *21*–*25*), come from the lowest 37 m of the Willwood formation. Nineteen species are represented among 233 specimens, including diagnostic Wa-0 taxa (*Arfia junnei*, *Copecion davisi*, *Hyracotherium sandrae*, and *Diacodexis ilicis*) (*25*). The lowest Wa-0 fossils come from paleosols and clay clast accumulations in sandstones 3 to 5 m above the base of the Willwood formation and 8 m above the highest Clarkforkian mammals. The highest Wa-0 fossils occur 37 m above the base of the Willwood formation and 3 m below three thick, laterally persistent, red paleosols. In the Cabin Fork area, the highest of these three persistent paleosols (at 47 m) produced 10 species of mammals, including *Cardiolophus radinskyi*, which defines the succeeding Wa-1 faunal zone (*25*) (Fig. 2). Thus, the Wa-0 faunal zone in the Cabin Fork area is at least 34 m thick and is bounded by Cf-3 and Wa-1 faunas.

We measured the carbon isotopic composition of bulk organic matter ($\delta^{13}C_{org}$) from mud-rock paleosols in the same sections (*26*) (Fig. 2A and fig. S1). $\delta^{13}C_{org}$ ranged from –22 to –28.5 per mil (‰) and, when grouped into PETM and non-PETM samples based on faunal criteria, was strongly negatively correlated with the weight percent of organic carbon (wt % C_{org}), which varies from 3.6% to 0.05% (fig. S1 and table S1). We plotted deviations of $\delta^{13}C_{org}$ from the values expected based on wt % C_{org} (*26*) (Fig. 2A and fig. S1). The carbon isotope curve shows a sharp excursion of –3.3‰, starting 2 to 3 m below the lowest occurrence of Wa-0 mammals. The magnitude of the CIE is similar to that in soil organic matter at Polecat Bench in the northern Bighorn Basin (*27*) (Fig. 2B). Our isotope anomaly values remain 2 to 3‰ below background values throughout the 50 m of section above the base of the CIE, with the exception of a single more positive sample at 5 m (Fig. 2A) that was poorly consolidated and contaminated with modern roots. The lowest Wa-1 mammals occur within the upper part of the CIE, as is seen at Polecat Bench (*27*) (Fig. 2B).

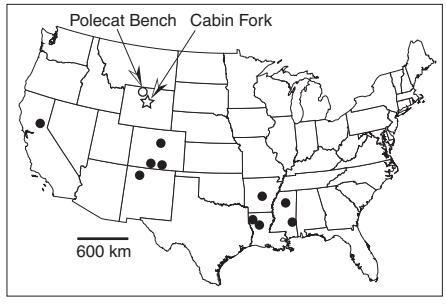

Fig. 1. The location of the Cabin Fork and Polecat Bench PETM sections. Solid dots indicate Paleocene and Eocene sites with plant types that are restricted to the PETM in northern Wyoming.

[1]Department of Paleobiology, Smithsonian Museum of Natural History, 10th Street and Constitution Avenue, NW, Washington, DC 20560, USA. [2]Department of Geography, Earth, and Environmental Sciences, University of Birmingham, Edgbaston, Birmingham B15 2TT, UK. [3]Department of Geosciences, The Pennsylvania State University, University Park, PA 16802, USA. [4]Division of Vertebrate Paleontology, Florida Museum of Natural History, 222 Dickinson Hall, Museum Road and Newell Drive, Gainesville, FL 32611, USA. [5]Department of Anatomical Sciences, Stony Brook University, Stony Brook, NY 11794–8081, USA.

*To whom correspondence should be addressed. E-mail: wings@si.edu

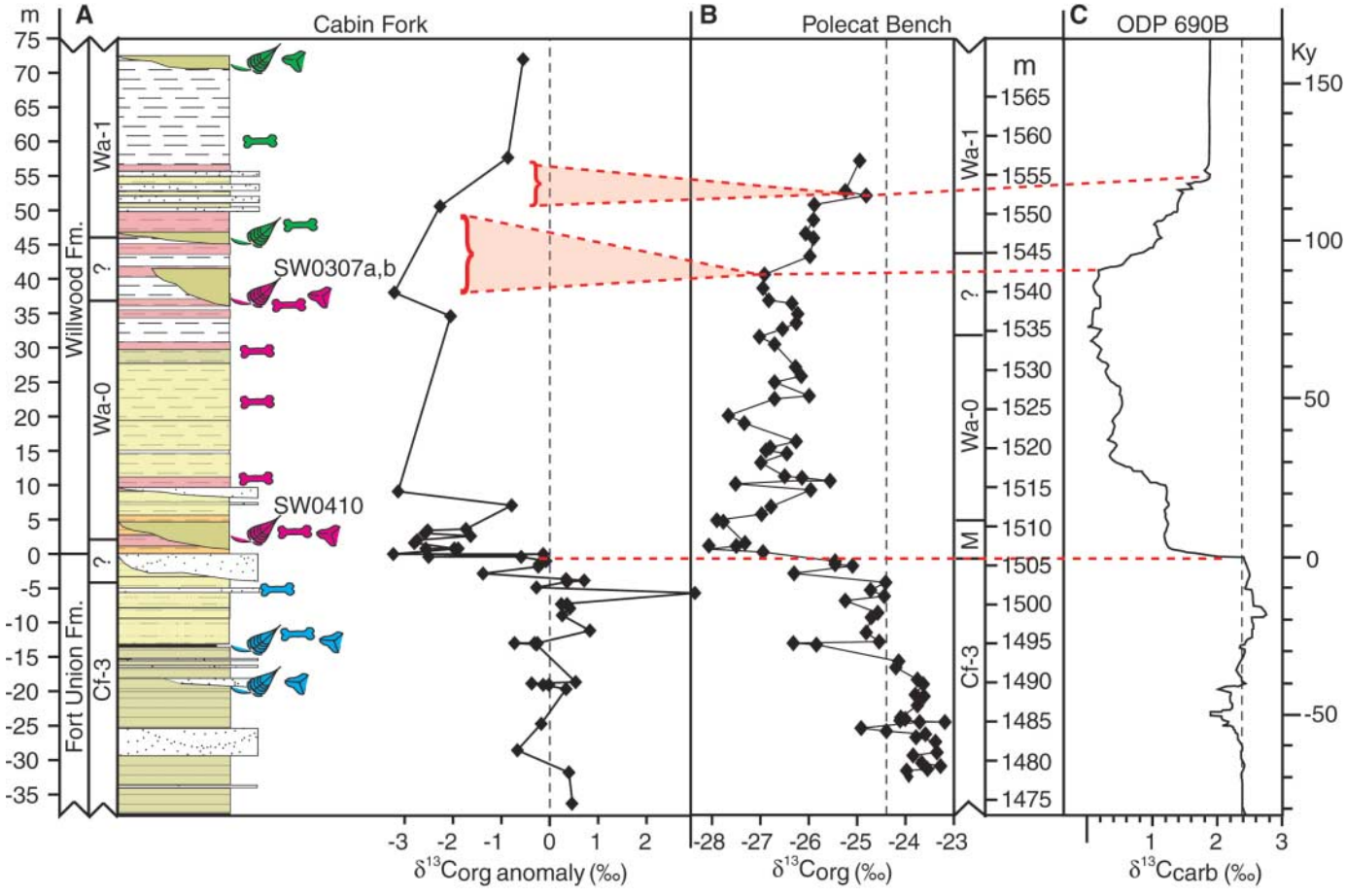

Fig. 2. Comparison of PETM records. (**A**) The Cabin Fork section, showing meter levels, formations, faunal zones, lithology, fossil sites, and $\delta^{13}C_{org}$ anomaly values (*26*). (**B**) The Polecat Bench section, showing $\delta^{13}C_{org}$, faunal zones, and meter levels (*27*). (**C**) $\delta^{13}C$ of bulk carbonate at Ocean Drilling Program (ODP) site 690B (in the Southern Ocean), with the time scale from Farley and Eltgroth (*3*). Wa, Wasatchian; Cf, Clarkforkian; M, *Meniscotherium* Zone. Paleocene fossils are indicated with blue symbols, PETM with red, and post-PETM Eocene with green. Carbon isotope units are in ‰ Pee Dee belemnite. Dashed orange lines indicate correlations of carbon isotope curves. Dashed vertical lines are mean $\delta^{13}C$ vales for the latest Paleocene.

Floral composition and migration. Plant fossils were collected from lenticular channel fills 3 to 5 m thick and <50 m across. Because of small-scale downcutting and redeposition, plant fossils are slightly younger than overbank deposits at the same level; however, the continuous floodplain paleosols above the channel fills are within the PETM, as indicated by vertebrate fossils and/or $\delta^{13}C_{org}$ anomaly values.

Two localities, SW0410 and SW0307 (3 and 37 m above the base of the CIE, respectively), produced a total of 398 plant megafossil specimens [136 and 262, respectively (table S3)]. The lower locality has nine leaf morphospecies, including six dicots, one palm, and one fern. The upper locality has 20 leaf morphospecies, including 17 dicots, one palm, and two ferns. In composition, both PETM megafloral localities are dominated by morphospecies that have not been recognized in extensive collections (~30,000 specimens from >300 localities) from the late Paleocene and early Eocene of the Bighorn Basin (Fig. 3) (*28*).

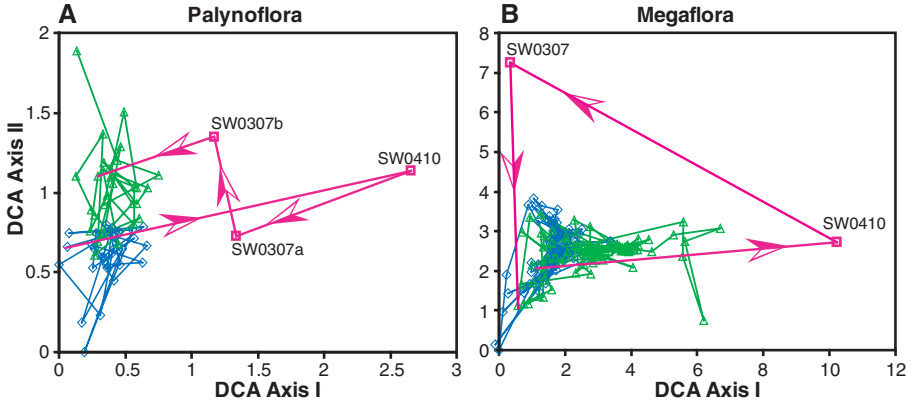

Fig. 3. Change in floral composition analyzed with detrended correspondence analysis (DCA). Each bivariate plot was generated by DCA of a sites-by-species matrix of presence/absence data. Arrows indicate the temporal sequence. (**A**) Palynofloral analysis: Axis I, 11.5% of variance; Axis II, 5% of variance. (**B**) Megafloral analysis: Axis I, 3% of variance; Axis II, 2% of variance. Paleocene samples are indicated with blue diamonds, Eocene samples with green triangles, and PETM samples with red squares. PETM samples are compositionally distinct from both Paleocene and Eocene ones and from each other.

The lower flora is dominated by an undescribed, mimosoid legume leaflet and contains leaves similar to "*Artocarpus*" *lessigiana* (Lesquereux) Knowlton, a taxon known from the Paleocene and Eocene of the Denver Basin, Mississippi Embayment, and California

(*29*), locations 650 to 1500 km to the south (Fig. 1 and fig. S2). The upper flora is co-dominated by an undescribed leaf of probable lauralean affinity with a long drip tip, a typical Paleocene lauralean known as "*Ficus*" *planicostata*, and the common late Paleocene–early Eocene platanoid *Macginitiea nobilis* (fig. S3).

Palynofloras extracted from the megafloral sites also have unusual floral composition compared to latest Paleocene and post-PETM samples from the same region (Fig. 3A) (*16*, *17*). Both palynofloras have common, stratigraphically long-ranging, wind-pollinated taxa (such as *Caryapollenites*, *Ulmipollenites*, and *Alnipollenites*), but the lower flora also includes *Brosipollis*, a marker of the early Eocene on the Gulf Coastal Plain (*30*, *31*); *Punctatosporites*, an Eocene index fossil in the Bighorn Basin; and four taxa not previously recorded among ~25,000 grains identified from the late Paleocene and earliest Eocene in the Bighorn Basin (*17*). The upper site contains ?*Lanagiopollis*, cf. *Tricolpites hians*, and *Platycarya swasticoides* (three forms otherwise restricted to the Gulf Coastal Plain); *Triporopollenites granulatus* and *Cycadopites scabratus* (both otherwise found in the Powder River and Williston Basins to the east); the Eocene index *Platycarya platycaryoides*; and four taxa previously unrecorded in the Bighorn Basin including cf. *Bombax* (*30*–*33*). As in the Powder River Basin, *P. platycaryoides,* which migrated to North America from Europe, does not appear until the upper part of the PETM, suggesting it may have not have colonized middle latitudes until climate began to cool late in the event (*19*).

The taxa found in these PETM floras are otherwise unknown from the northern Rocky Mountain region, and the four palynomorphs and one leaf type noted above document northward range extensions from the Gulf Coastal Plain and from Colorado (Fig. 1 and table S4). PETM occurrences of these taxa 650 to 1500 km north of their Paleocene distributions roughly indicate the magnitude of range extension, although incomplete knowledge of Paleocene distributions means these may be overestimates. Paleogene gradients of temperature with latitude have been estimated at 0.4 to 1°C change in mean annual temperature (MAT) per degree of latitude (*34*, *35*). A temperature increase of 4 to 8°C during the PETM (*36*) should have shifted floral ranges 4 to 20 degrees of latitude (450 to 2200 km) to the north, which agrees with the range extensions we infer.

The combination of immigrants from the south, east, and Europe, along with the persistence of natives, is consistent with species-specific, or "individualistic," response to the PETM, as has been widely reported in late and postglacial floras (*37*). The presence of immigrants in the lowest PETM flora suggests that plant range changes were geologically rapid (<10 ky from the base of the CIE). The absence of a distinctive PETM flora in earlier studies probably reflects inadequate sampling (*17*, *19*) or limited change in floral ranges on isolated land masses (*18*). The appearance during the PETM of both intra- and intercontinental floral immigrants mirrors the pattern seen in the fauna, which includes both intracontinental (*Meniscotherium*) and intercontinental (hyaenodontid creodont) migrants (*14*, *21*).

Paleoclimate. Leaf margin analysis (LMA) (*38*, *39*) of the 23 dicot leaf morphospecies from the two localities yielded a MAT estimate of 19.8 ± 3.1°C for the PETM [the error is 1 SD, following Wilf (*39*)]. This is 4.9°C higher than the MAT (15.7 ± 2.4°C) estimated from LMA of floras from the 250-ky interval immediately before the PETM in the same region and 1.6°C higher than the MAT (18.2 ± 2.3°C) for the 400-ky interval after the PETM (*40*). Oxygen isotopic composition of biogenic apatite from the Bighorn Basin indicates even higher temperature during the PETM (26°C) (*35*). Modern riparian and wetland vegetation has a higher proportion of toothed species than terra firma forest, commonly resulting in 2.5 to 7°C underestimates of MAT (*41*, *42*). All the fossil floras used to estimate MAT were deposited in fluvial backswamps or channel margins (*28*); paleotemperature estimates are therefore likely to be uniformly low. However, the ~5°C warming estimated from LMA is consistent with isotopic temperature estimates.

We used leaf area analysis (LAA) (*43*) to estimate mean annual precipitation (MAP) at 123 cm (the standard error of the regression is +177/–86 cm) for the combined PETM flora. A different regression derived from a modern data set with more dry sites (*44*) yielded an MAP estimate of 120 cm. The marked increase in leaf size from the lower to the upper PETM megaflora (figs. S2 and S3) led us to estimate MAP separately for each site. By using the two regressions (*43*, *44*) we estimate a MAP of 80 +114/–56 cm and 41 cm for the lower flora. MAP estimates for the upper flora were 144 +206/–100 cm and 132 cm. Although the MAP estimate for the lower flora was derived from only six morphospecies, the two with the smallest leaves (nanophyll-microphyll) are also the most abundant, indicating that small-leaved species were local dominants. MAP estimates for the late Paleocene in southern Wyoming average 138 cm (*45*), suggesting that rainfall declined by ~40% near the onset of the PETM then recovered to normal values by late in the event. A warm, wet climate late in the PETM is consistent with the exceptionally thick paleosols preserved from the upper part of the event (Fig. 2) (*46*).

Previous studies of the PETM have yielded mixed evidence for precipitation change. A higher abundance of terrestrial palynomorphs and eutrophic dinoflagellates in nearshore marine sediments has been cited as evidence of more runoff and higher precipitation (*18*, *47*), as has the greater magnitude of the CIE in pedogenic carbonate nodules than in marine carbonates (*48*). In contrast, the continental record of the PETM in Spain suggests a persistently or seasonally dry climate (*49*), and a possible PETM section in southern England has exceptional amounts of fossil charcoal (*50*).

Without wider geographic coverage, we do not know if the short period of dry climate we infer at the onset of the PETM is regional or global. However, even if it was confined to the northern Rocky Mountain region, it could have had an important positive feedback on climate by increasing the likelihood of burning in the extensive upper Paleocene peats and coals of the Powder River Basin (*9*).

Conclusion. The PETM provides an important analog to present-day anthropogenic global warming, because the two episodes are inferred to have similar rates and magnitudes of carbon release and climate change (*6*). In this context, it is notable that terrestrial floras underwent rapid (within ~10 ky), individualistic range change during the PETM, including both intra- and intercontinental migration. Plant range changes of similar scale may occur with anthropogenic climate change. Fossils revealing this dramatic, transient, floral response to PETM warming eluded years of focused searching, suggesting that other such short-term shifts in floral composition remain to be uncovered from the "deep time" record of ecological change.

References and Notes

1. J. C. Zachos *et al.*, *Science* **302**, 1551 (2003).
2. U. Röhl, T. J. Bralower, R. D. Norris, G. Wefer, *Geology* **28**, 927 (2000).
3. K. A. Farley, S. F. Eltgroth, *Earth Planet. Sci. Lett.* **208**, 135 (2003).
4. F. M. Gradstein *et al.*, *A Geologic Time Scale 2004* (Cambridge Univ. Press, Cambridge, 2004).
5. The PETM is also known as the Initial Eocene Thermal Maximum (IETM).
6. J. C. Zachos *et al.*, *Science* **308**, 1611 (2005).
7. G. R. Dickens, J. R. O'Neil, D. K. Rea, R. M. Owen, *Paleoceanography* **10**, 965 (1995).
8. H. Svensen *et al.*, *Nature* **429**, 542 (2004).
9. A. C. Kurtz, L. R. Kump, M. A. Arthur, J. C. Zachos, A. Paytan, *Paleoceanography* **18**, 1090 (2003).
10. E. Thomas, in *Late Paleocene–Early Eocene Climatic and Biotic Events in the Marine and Terrestrial Records*, M.-P. Aubry, W. A. Berggren, S. Lucas, Eds. (Columbia Univ. Press, New York, 1998), pp. 214–243.
11. D. C. Kelly, *Paleoceanography* **17**, 1071 (2002).
12. E. M. Crouch *et al.*, *Geology* **29**, 315 (2001).
13. W. C. Clyde, P. D. Gingerich, *Geology* **26**, 1011 (1998).
14. G. J. Bowen *et al.*, *Science* **295**, 2062 (2002).
15. S. L. Wing, in *Late Paleocene–Early Eocene Climatic and Biotic Events in the Marine and Terrestrial Records*, M.-P. Aubry, W. A. Berggren, S. Lucas, Eds. (Columbia Univ. Press, New York, 1998), pp. 380–400.

16. G. J. Harrington, *U. Mich. Pap. Paleontol.* **33**, 89 (2001).
17. S. L. Wing, G. J. Harrington, *Paleobiology* **27**, 539 (2001).
18. E. M. Crouch, H. Visscher, *Geol. Soc. Am. Spec. Pap.* **369**, 333 (2003).
19. S. L. Wing, G. J. Harrington, G. J. Bowen, P. L. Koch, *Geol. Soc. Am. Spec. Pap.* **369**, 425 (2003).
20. K. D. Rose, *U. Mich. Pap. Paleontol.* **26**, 1 (1981).
21. P. D. Gingerich, *U. Mich. Pap. Paleontol.* **33**, 37 (2001).
22. P. L. Koch, J. C. Zachos, D. L. Dettmann, *Palaeogeogr. Palaeoclimatol. Palaeoecol.* **115**, 61 (1995).
23. G. J. Bowen *et al.*, *U. Mich. Pap. Paleontol.* **33**, 73 (2001).
24. S. G. Strait, *U. Mich. Pap. Paleontol.* **33**, 127 (2001).
25. P. D. Gingerich, *U. Mich. Pap. Paleontol.* **28**, 1 (1989).
26. Materials and methods are available as supporting material on *Science* Online.
27. R. Magioncalda, C. Dupuis, T. Smith, E. Steurbaut, P. D. Gingerich, *Geology* **32**, 553 (2004).
28. S. L. Wing, J. Alroy, L. J. Hickey, *Palaeogeogr. Palaeoclimatol. Palaeoecol.* **115**, 117 (1995).
29. R. W. Brown, *U.S. Geol. Surv. Prof. Pap.* **375**, 1 (1962).
30. G. J. Harrington, *Palaios* **16**, 266 (2001).
31. G. J. Harrington, *Geol. Soc. Am. Spec. Pap.* **369**, 381 (2003).
32. G. J. Harrington, S. J. Kemp, *Palaeogeogr. Palaeoclimatol. Palaeoecol.* **167**, 1 (2001).
33. G. J. Harrington, S. J. Kemp, P. L. Koch, *J. Geol. Soc. (London)* **161**, 173 (2004).
34. D. R. Greenwood, S. L. Wing, *Geology* **23**, 1044 (1995).
35. H. C. Fricke, S. L. Wing, *Am. J. Sci.* **304**, 612 (2004).
36. H. C. Fricke, W. C. Clyde, J. R. O'Neil, P. D. Gingerich, *Earth Planet. Sci. Lett.* **160**, 193 (1998).
37. S. T. Jackson, J. T. Overpeck, *Paleobiology* **26** (suppl.), 194 (2000).
38. J. A. Wolfe, *U.S. Geol. Surv. Prof. Pap.* **1106**, 1 (1979).
39. P. Wilf, *Paleobiology* **23**, 373 (1997).
40. S. L. Wing, H. Bao, P. L. Koch, in *Warm Climates in Earth History*, B. T. Huber, K. MacCleod, S. L. Wing, Eds. (Cambridge Univ. Press, Cambridge, 2000), pp. 197–237.
41. R. J. Burnham, N. C. Pitman, K. R. Johnson, P. D. Wilf, *Am. J. Bot.* **88**, 1096 (2001).
42. E. A. Kowalski, D. L. Dilcher, *Proc. Natl. Acad. Sci. U.S.A.* **100**, 167 (2003).
43. P. Wilf, S. L. Wing, D. R. Greenwood, C. L. Greenwood, *Geology* **26**, 203 (1998).
44. B. F. Jacobs, P. S. Herendeen, *Palaeogeogr. Palaeoclimatol. Palaeoecol.* **213**, 115 (2004).
45. P. Wilf, *Geol. Soc. Am. Bull.* **112**, 292 (2000).
46. T. M. Bown, M. J. Kraus, *Palaios* **8**, 68 (1993).
47. E. M. Crouch *et al.*, *Palaeogeogr. Palaeoclimatol. Palaeoecol.* **194**, 387 (2003).
48. G. J. Bowen, D. J. Beerling, P. L. Koch, J. C. Zachos, T. Quattlebaum, *Nature* **432**, 495 (2004).
49. B. Schmitz, V. Pujalte, *Geology* **31**, 689 (2003).
50. M. E. Collinson, J. J. Hooker, D. R. Gröcke, *Geol. Soc. Am. Spec. Pap.* **369**, 333 (2003).
51. We thank P. Wilf, R. Secord, and G. Bowen for comments and the Biological Complexity of the Paleocene-Eocene Boundary (BIOPE) group for discussion. Supported by NSF grant nos. EAR–0120727 and EAR-0308902, the Roland Brown Fund, and the Florida Museum of Natural History. This is publication no. 146 of the Smithsonian Evolution of Terrestrial Ecosystems Program.

Supporting Online Material
www.sciencemag.org/cgi/content/full/310/5750/993/DC1
Materials and Methods
Figs. S1 to S3
Tables S1 to S4
References and Notes

5 July 2005; accepted 10 October 2005
10.1126/science.1116913

Obestatin, a Peptide Encoded by the Ghrelin Gene, Opposes Ghrelin's Effects on Food Intake

Jian V. Zhang, Pei-Gen Ren, Orna Avsian-Kretchmer, Ching-Wei Luo, Rami Rauch, Cynthia Klein, Aaron J. W. Hsueh*

Ghrelin, a circulating appetite-inducing hormone, is derived from a prohormone by posttranslational processing. On the basis of the bioinformatic prediction that another peptide also derived from proghrelin exists, we isolated a hormone from rat stomach and named it obestatin—a contraction of obese, from the Latin "obedere," meaning to devour, and "statin," denoting suppression. Contrary to the appetite-stimulating effects of ghrelin, treatment of rats with obestatin suppressed food intake, inhibited jejunal contraction, and decreased body-weight gain. Obestatin bound to the orphan G protein–coupled receptor GPR39. Thus, two peptide hormones with opposing action in weight regulation are derived from the same ghrelin gene. After differential modification, these hormones activate distinct receptors.

The increasing prevalence of obesity is a global problem. Body weight is regulated in part by peptide hormones produced in the brain or gut or both (*1*). Earlier studies on synthetic and peptidyl growth hormone (GH) secretagogues (*2*–*4*) led to the identification of a specific G protein–coupled receptor (GPCR), the GH secretagogue receptor (GHSR) (*5*, *6*), and subsequently to the discovery of its endogenous ligand, ghrelin (*7*), a gut-derived circulating hormone that stimulates food intake (*4*, *8*).

Human ghrelin, a 28–amino acid peptide, is derived by posttranslational cleavage from a prepropeptide of 117 residues. On the basis of bioinformatic searches of putative hormones derived from the prepropeptides of known peptide hormones, we identified a ghrelin-associated peptide. We searched GenBank for orthologs of the human ghrelin gene and compared preproghrelin sequences from 11 mammalian species. In addition to the known ghrelin mature peptide, which immediately follows the signal peptide, we identified another conserved region that was flanked by potential convertase cleavage sites (fig. S1, underlined). This region encodes a putative 23–amino acid peptide, with a flanking conserved glycine residue at the C terminus, suggesting that it might be amidated (*9*). We named this ghrelin-associated peptide obestatin.

Division of Reproductive Biology, Department of Obstetrics and Gynecology, Stanford University School of Medicine, Stanford, CA 94305–5317, USA.

*To whom correspondence should be addressed: E-mail: aaron.hsueh@stanford.edu

Characterization of endogenous obestatin. To detect endogenous obestatin, we prepared a synthetic obestatin peptide and performed radioimmunoassays on rat-tissue extracts with obestatin-specific antibodies. As shown in Fig. 1A, the stomach extract displaced I^{125}-obestatin binding to the obestatin antibodies. Obestatin-like activities from stomach extracts were purified. Immunoreactive (ir) obestatin was eluted in a Sephadex G-50 gel permeation column (Amersham Biosciences, Piscataway, NJ) with estimated sizes of 2.6 and 1.5 kilodaltons (kD), distinct from the elution position of mature ghrelin (Fig. 1B). We subjected peak 1 (2.6 kD) fractions to ion-exchange fast protein liquid chromatography (FPLC). A single peak of ir obestatin was eluted (Fig. 1C) and shown by mass spectrometry and Edman sequencing to contain a peptide with a molecular mass of 2516.3 (Fig. 1D) and with a sequence of FNAPFDVGIKLSGAQYQQHG-XX (*10*). Combined with molecular-weight determination, the full sequence of the purified peptide was predicted to be FNAPFDVGIKLSGAQYQQHGRAL-NH_2, consistent with the obestatin sequence deduced from rat ghrelin cDNA. In addition, mass spectrometric analyses suggested that peak 2 (1.5 kD) represented the last 13 residues of amidated obestatin, indicating further processing.

To investigate differential secretion of ghrelin and obestatin in vivo, we fasted adult male rats for 48 hours before refeeding. Consistent with earlier findings (*11*), fasting led to a major increase in serum ghrelin levels, whereas subsequent refeeding for 2 hours by allowing animals free access to food or drinking water containing dextrose decreased circulating ghrelin (Fig. 1E). In contrast, serum levels of obestatin determined by a radioimmunoassay were constant in the different treatment groups.